Fractionation of softwood fiber (TMP) using a rotating cone

VILAS B. REWATKAR AND JACOB H. MASLIYAH

ABSTRACT

A rotating cone was used to fractionate fibers from a 100% softwood pulp at a consistency of 0.95% ± 0.02%. The rotating cone fractionators used in this study had two unique features: (a) their surfaces were constructed from a sieve mesh, thereby introducing a "rough" surface, and (b) the point of feed delivery was offset from the cone's axis of rotation. Six fractions were collected at different angular positions in a specially designed collection assembly. Fractionation performance was enhanced by aligning the first collection zone with the dispersed spray originating at the transition boundary on the rim of the cone. The design parameters of the cone (surface roughness, cone angle, and cone diameter) were studied in detail. The design of the feed distributor (shape and opening area) was also studied. Results showed that the best fractionation performance was obtained using cones with an angle of 30° made from 20-mesh screens. A large, elliptically shaped feed distributor gave the best fractionation performance. The results suggest the possibility of scale-up based on constant tip speed at a given flow rate.

Application:

A new approach to fiber fractionation

In an earlier study *(1)*, fiber fractionation using rotating cone fractionators was found to be superior to the conventional plate atomizing wheel proposed in the literature *(2–9)*. The unique features of the rotating cone fractionator adopted in this study were that (a) its surface was constructed from a sieve mesh, thereby producing a "rough" surface, and (b) the location of the feed pipe was offset from the cone's axis of rotation. Our experimental conditions were at variance with those used in the literature (i.e., lower rotational speed, nonuniform feed rate, and rough surface). Fractionated products were collected at several angular locations in a specially designed collection assembly. The results from the previous study *(1)* suggested that a rotating cone fractionator operating at minimal rotational speeds can fractionate 100% hardwood fibers according to length and percentage of fines associated with them.

In the present study, a new method of aligning the collection zones with the dispersed spray is proposed to maximize fractionation efficiency. An attempt was made to enhance fiber fractionation performance by investigating the influence of the design parameters of the rotating cone fractionator. The effect of surface roughness, cone angle, and cone diameter were studied in detail. The effect of design details for the feed distributor, such as shape and distributor area, were also studied at some length. Finally, the effect of feed flow rate and rotational speed were studied for the optimum cone design and feed distributor.

The experimental results are presented in three ways:

1. Variation of average fiber length within the six collection zones
2. Variation of average fiber length of cumulative mixtures of different fractions
3. Extent of fractionation.

EXPERIMENTAL SETUP AND PROCEDURE

Figure 1 shows a schematic diagram of the experimental setup used in this study. A fiber suspension of 100% softwood thermomechanical (TMP) (supplied by Paprican, UBC, BC) was prepared in a feed storage tank and maintained in a well-mixed condition with the help of a stirrer. The fiber suspension was pumped using a progressing cavity pump and fed to the rotating conical surface at a constant flow rate. Feed flow rate was measured using a precalibrated magnetic flow meter. In all cases, the feed delivery point was offset from the cone's axis of rotation.

The feed fiber suspension flowed over the conical surface, and at the rim of the cone it was dispersed into the air. The dispersed spray was collected in a specially designed collection assembly placed concentric to the rotating cone. **Figure 2** provides top views showing two types of zone alignment of the collection assembly with respect to the dispersed spray. The collection assembly was made up of six equally spaced compartments built within a cylindrical vessel. The bottom of the cylindrical vessel was an inverted cone, which facilitated removal of the fiber suspensions. Each compartment (or collection zone) was provided with its own outlet at the bottom of the vessel. Most experiments were carried out by adjusting the collection assembly such that the dispersed spray from the transition arc boundary at the rim of the cone was captured by the first collection zone, as shown in Fig. 2a. When a cone diameter of 180

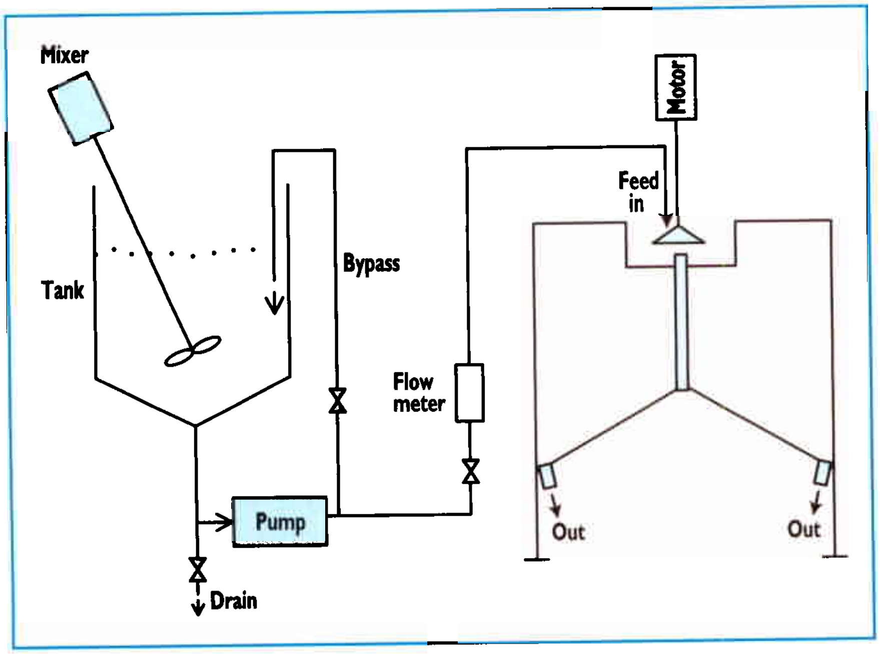

1. Experimental setup

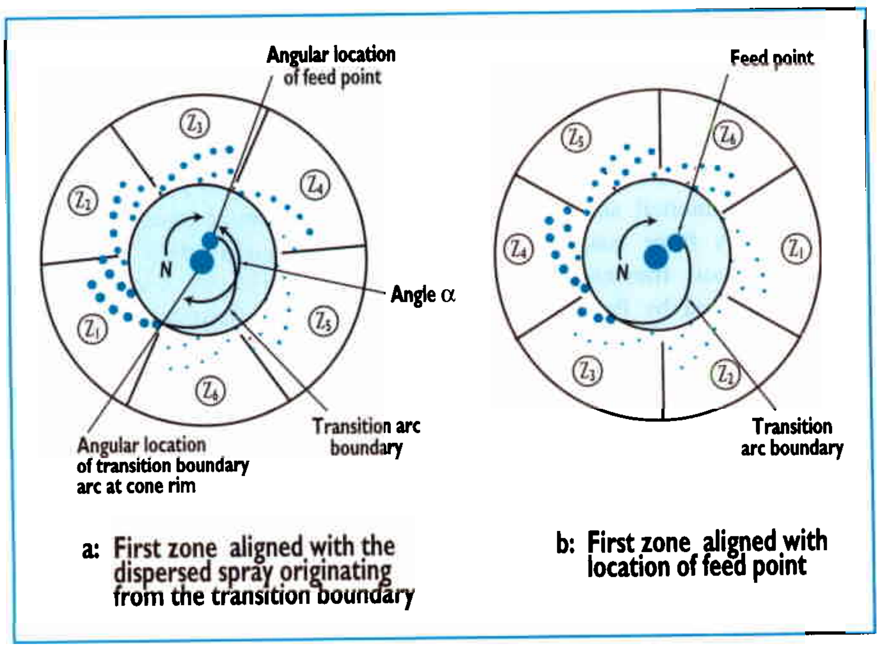

2. Top views of the two zone alignments of the collection assembly

mm was used, the annular gap between the cone rim and inner boundary of the collection chambers (200 mm) was small. Under this situation, the angular location of the transition arc boundary at the rim of the cone is aligned with the angular location of the leading edge of the first collection zone. Few tests were carried out by aligning the first collection zone with the angular location of feed point (as shown in Fig. 2b), as was done in the earlier study *(1)*. The subsequent zone numbers were assigned based on their angular location compared with the location of the first collection zone.

Design details of the rotating cone and the feed distributor are given in **Fig. 3** and **Table I**. The major axis of the elliptically shaped distributor was aligned with the axis of rotation. In the majority of experiments, the radial location of the distributors was 30 mm away from the axis of rotation. Cones were fabricated using different mesh screens. The details of wire size and opening for these mesh sieve screens are given in **Table II**. The holes of a mesh sieve were blocked using adhesive tape on the lower side of the cone surface, so that no suspension can pass directly through the holes.

A fiber quality analyzer (FQA) (OpTest Equipment Inc., Hawkesbury, ON) was used to measure the average fiber length and percentage of fines (L < 0.2 mm) present in the feed and the collected fractions. For a given sample, an FQA provides three types of mean fiber lengths:

1. Arithmetic mean length L_A

$$L_A = \frac{\sum n_j L_j}{\sum n_j} \quad (1)$$

2. Length-weighted mean length L_L

$$L_L = \frac{\sum n_j L_j^2}{\sum n_j L_j} \quad (2)$$

3. Weight-weighted mean length L_W

$$L_W = \frac{\sum n_j L_j^3}{\sum n_j L_j^2} \quad (3)$$

where

j = 1, 2, …, n
n = fiber count
L = measured fiber length (contour length)

In the present study, data of length-weighted mean length L_L was used.

For a given experimental run, the amount of fiber suspension collection in each zone was measured (weight basis). The consistency of the fiber suspension was calculated using TAPPI T 240 om-88 *(10)*. The dry weight of fibers in the fiber suspension was calculated as the product of the weight of fiber suspension and its corresponding consistency. The fraction of feed collected (based on dry weight of fibers) in each zone was calculated by taking the ratio of the dry weight of fibers collected for an individual zone to the total dry weight of fibers in the feed.

In order to measure quantitatively the extent of fractionation, the following method was used. Letting $L_{L,i}$ be the average fiber length of sample i (samples collected from Zones 1-6) for which the weight fraction of feed fibers collected is x_i, then the average length for the set of all six zones is given by:

$$L_{LF} = \sum_{i=1}^{6} x_i L_{L,i} \quad (4)$$

The extent of fractionation ΔL_L is a measure of the difference in fiber length between the zones. This important quantity is defined in Eq. 5:

$$\Delta L_L = \left[\sum_{i=1}^{6} x_i \left(L_{L,i} - L_{LF} \right)^2 \right]^{1/2} \quad (5)$$

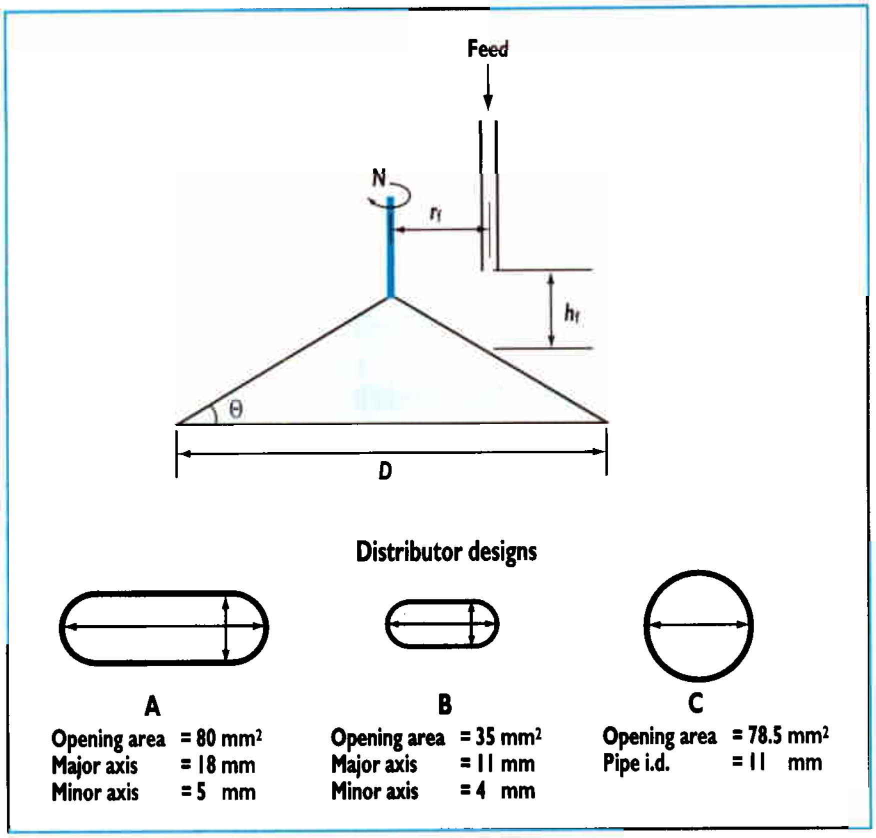

3. Design details of cone, feed pipe location, and distributor

The fractionation results obtained under different test conditions were compared based on the calculated values of ΔL_L.

Pulp type	100% softwood (TMP)
Feed average fiber length	L_A = 0.57 mm
	L_L = 1.37 mm
	L_W = 2.08 mm
Feed consistency	X = 0.95 ± 0.02%
Design details of cone	Angle = 15°, 30°, 45°, 60°
	D = 120 mm, 180 mm
	Surface roughness = 0, 12, 20, 32 mesh screen
Feed distributor	
A	elliptical area = 80.0 mm²
B	elliptical area = 35.0 mm²
C	circular area = 78.5 mm²
Feed location	h_f = 10 mm
	r_f = 30 mm
Rotational speed	N = 300, 450, 600, 670 rpm
Feed flow rate	Q = 1.5, 2.6, 4.2, 7.0 × 10^{-5} m³/s
Fiber count for average fiber length	n = 4000

I. Experimental conditions

RESULTS AND DISCUSSION

General discussion

The fractionation results are presented in three ways:

1. Variation of average fiber length within each of the six collection zones
2. Variation of average fiber length for cumulative mixtures of different fractions
3. Extent of fractionation.

Variation of average fiber length within the collection zones. The measured values of average fiber length for the samples collected in the various compartments or zones were plotted against the collection zone number. For a given set of test conditions, fractionation occurred along the periphery of the cone, whereby the collected fibers had different average fiber length at the various collection zones. If the dispersed spray originating from the transition boundary at the cone rim was captured in the first zone of the collection assembly (Fig. 2a), then the fiber length continuously decreased from Zone 1 to Zone 6. In a few experiments, the fiber length values of Zone 5 were slightly higher than Zone 6. This was due to large fluctuation in the location of the transition arc during the experiments.

Variation of average length for cumulative mixtures of different fractions. In order to compare the fractionation performance under different design and operating conditions, the average fiber length for cumulative collected fractions of increasing fiber length was plotted against the cumulative amount of fiber collected.

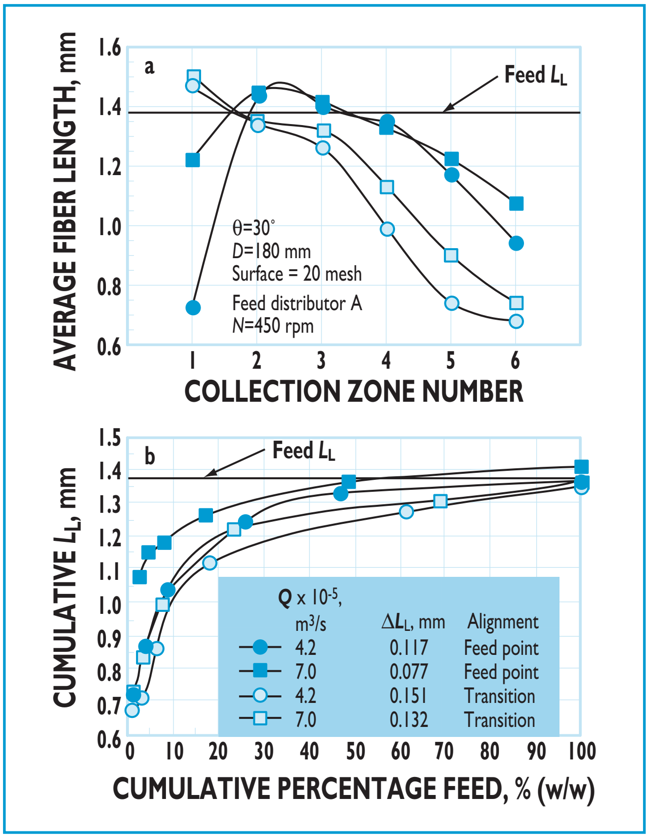

4. a: ***Average fiber length in the six collection zones and*** b: ***fractionation performance for two types of zone alignment***

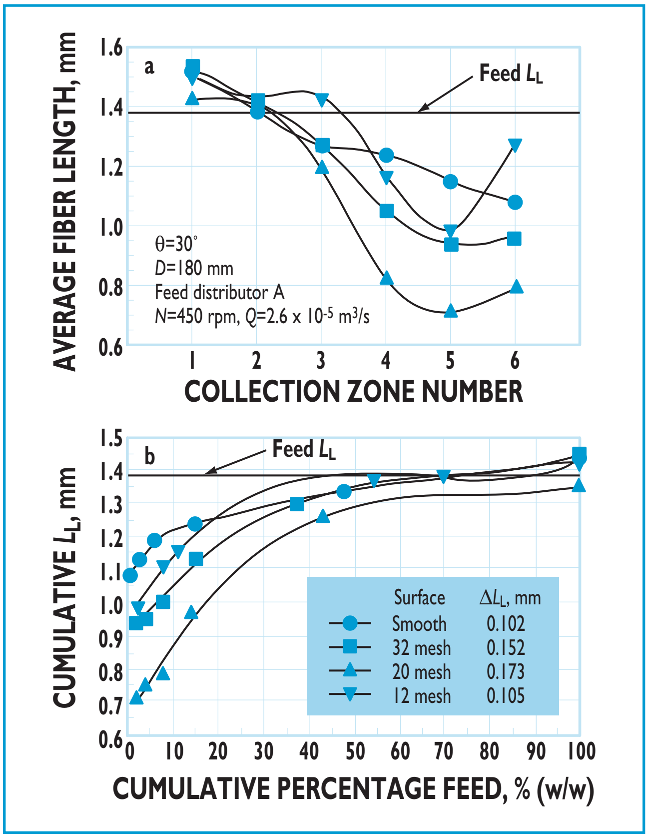

5. a: ***Average fiber length in the six collection zones and*** b: ***fractionation performance at different levels of cone roughness***

Screen size	Wire diameter, µm	Opening, µm
12 mesh	600	1710
20 mesh	474	798
32 mesh	237	553

II. Details of wire size and opening of the different screens

against the cumulative amount of fiber collected. The average fiber length was evaluated as if one were to mix the collected fractions of increasing fiber lengths.

The value of the average fiber length calculated for a mixture of all the fractions (i.e., at 100% cumulative feed) should approach the experimentally measured value of the feed average fiber length. The accuracy of analysis and sampling would thus manifest itself in the plot of cumulative values.

Extent of fractionation. The quantitative values for the extent of fractionation ΔL_L were calculated using the procedure discussed in the experimental section (Eq. 5). Values of ΔL_L were compared for different test conditions. In general, higher values of ΔL_L indicate larger differences in length between the collected fractions.

Comparison of fractionation performance for two different types of zone alignment

A rotating cone (30° cone angle, 180-mm diam.) was used in tests to evaluate fiber fractionation performance for the two different types of zone alignment. The angular location of the first zone within the collection assembly was aligned in one of two ways:

1. Transition boundary: Zone 1 aligned with the dispersed spray originating from the transition boundary at the cone rim (Fig. 2a)
2. Feed point: Zone 1 aligned with angular location of the feed point (Fig. 2b).

Experimental results for fiber fractionation obtained with the two types of zone alignment are given in **Fig. 4**. As seen in Fig. 4a, the average fiber length decreased continuously from Zone 1 to Zone 6 for the fractions collected using the transition alignment. With the feed-point alignment, fiber length increased from Zone 1 to Zone 2 and then decreased continuously through Zone 6.

With the feed-point alignment, the variation in fiber length with respect to zone location depended on the angular location of the transition boundary at the rim of the cone, which in turn varied with the design and operating parameters of the rotating cone. If the dispersed spray originating from the transition boundary happens to be aligned with the start of the second zone location, then maximum fiber length is obtained in the second zone.

(Fig. 2b), then the corresponding zone has a mixture of dispersed spray of long and short fibers. This decreases the maximum and increases the minimum values of average fiber length for the fractions collected in the adjacent zones.

Figure 4b plots the average fiber length of cumulative collected fractions (of increasing fiber length) against the cumulative amount of fiber collected. This plot is useful for evaluating the fractionation performance for the two types of zone alignment. The results show that when Zone 1 was aligned with the spray originating from the transition boundary, the fractionation performance was better than when Zone 1 was aligned with the angular location of the feed distributor. A large improvement was observed at a feed flow rate of 7.0 × 10^{-5} m^3/s. From the values of ΔL_L at a given flow rate (given in the legend of Fig. 4), it is clear that the transition type of zone alignment gave higher values than the feed-point type of zone alignment.

These observations led to the conclusion that the spray from the rotating cone with eccentric feed location shows a systematic variation in fiber length, with the highest length at the transition boundary, and it decreases continuously along the rim of the cone in the direction of rotation. Hence, better fractionation performance is obtained by aligning the angular location of the first collection zone with the spray originating from the transition boundary at the rim of the cone.

Cone angle (θ), degrees	Surface roughness, screen mesh	Cone speed (*N*), rpm	Flow rate (*Q*), 10^{-5} m^3/s	Angle (α), degrees
15	20	450	4.2	**94.5**
30	20	450	4.2	**93.0**
45	20	450	4.2	**116.5**
60	20	450	4.2	**160.2**
15	20	450	7.0	**67.4**
30	20	450	7.0	**61.4**
45	20	450	7.0	**67.3**
60	20	450	7.0	**118.3**
30	**none**	450	2.6	**57.4**
30	**12**	450	2.6	**158.3**
30	**20**	450	2.6	**122.8**
30	**32**	450	2.6	**115.0**
30	20	450	1.5	**173.0**
30	20	300	**2.6**	**83.7**
30	20	300	**4.2**	**63.3**
30	20	600	**2.6**	**146.0**
30	20	600	**4.2**	**104.6**

* Constant feed location; *D* = 180 mm; feed distributor A

***III. Values of α at different experimental conditions* ***

Variation of angular location of transition boundary with various operating parameters

Most of the experiments were carried out by adjusting the collection assembly such that the dispersed spray originating from the transition arc boundary at the rim of the cone was captured by the first zone. When the cone diameter of 180 mm was used, the annular gap between the cone rim and the inner boundary of the collection chambers (200 mm) was very small. Under this situation, the leading edge of the first collection zone can be aligned with the angular location of the transition arc boundary at the rim of the cone. Therefore, it seemed useful to identify the angular location of the transition boundary α (angle between the angular location of the feed distributor and the transition boundary at the rim of cone) for various design and operating parameters of the rotating cone fractionator.

Table III shows the measured values of α under several test conditions. From Table III, it is clear that the angular location of the transition boundary varied with the surface roughness, the cone angle, the rotational speed, and the feed flow rate. At a given flow rate, rotational speed, and cone angle, the value of α for different surface roughness increased in the following order: smooth < 32 mesh < 20 mesh < 12 mesh.

For a 20-mesh surface, the 30° cone angle gave the lowest value of α. Increasing or decreasing the cone angle led to a higher value of α. For all of the cone angles tested, at a constant rotational speed, α decreased with increasing feed flow rate. At a constant flow rate, α increased with increasing cone rotational speed.

The design and operating parameters influence the radial and angular velocity components of the flowing suspension, which in turn affect the angular location of the transition boundary at the rim of the cone. When a design or operating parameter increases the angular component of the resultant velocity, then the transition boundary shifts in the direction of rotation, consequently increasing α. If the angular velocity component (at higher rotational speeds) is fairly high, there will be some mixing or overlapping of incoming feed with fractionated suspension on the cone surface. Fractionation performance declines under such flow conditions *(1)*. When a design or operating parameter has the effect of increasing the radial velocity component, then the transition boundary shifts in the opposite direction of the cone rotation, resulting in a decrease in α. If the radial velocity component is fairly high (at high flow rates), the fiber suspension forms a film around the rim of the cone, which degrades fractionation performance.

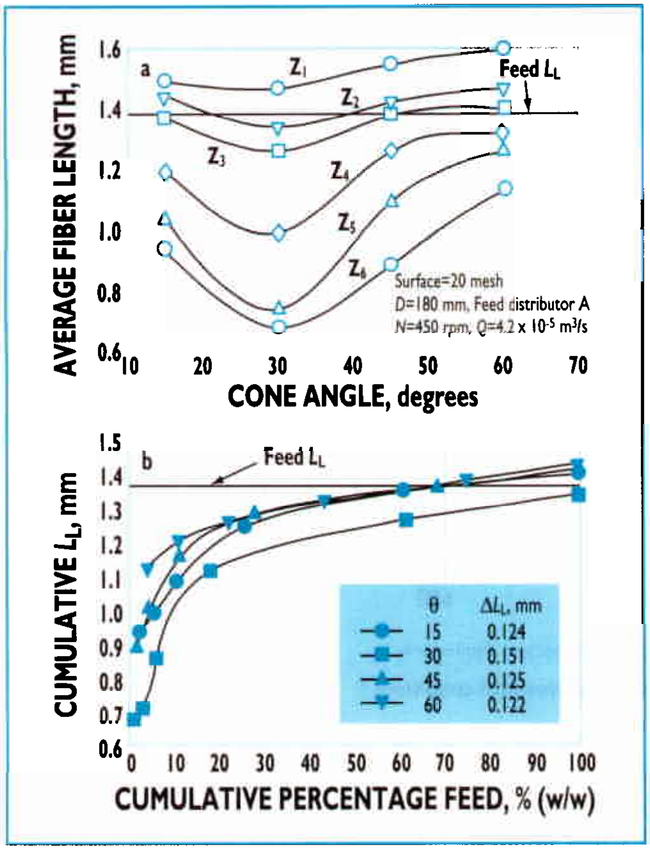

6. a: ***Average fiber length in the six collection zones and*** b: ***fractionation performance at different cone angles (Q = 4.2×10⁻⁵ m³/s)***

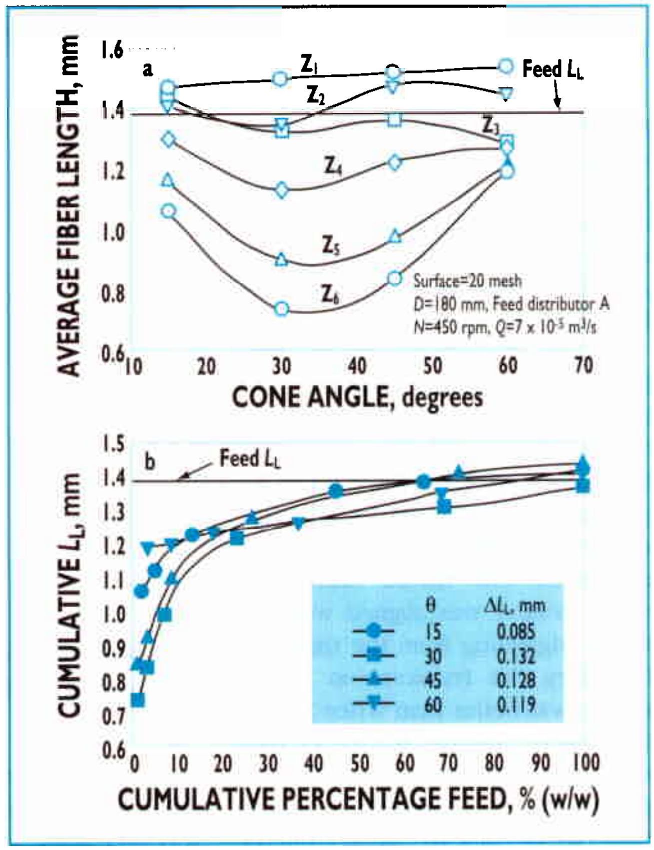

7. a: ***Average fiber length in the six collection zones and*** b: ***fractionation performance at different cone angles (Q = 7.0×10⁻⁵ m³/s)***

Effect of cone surface roughness

The effect of cone surface roughness was studied at a feed flow rate of 2.6 $\times 10^{-5}$ m^3/s and at a cone rotational speed of 450 rpm. The cones (180-mm diam., 30° angle) were fabricated using 12-, 20-, and 32-mesh sieve screens. The details of wire size and opening for the mesh sieve screens are given in Table II.

Figure 5 shows the experimental results for fiber fractionation at different levels of cone roughness. Figure 5a shows the average fiber lengths for the samples collected in each of the six collection zones. In all of the experimental runs, the average fiber length decreased continuously from Zone 1 to Zone 5. However, in three of the four runs, the average fiber length for Zone 6 was higher than in Zone 5. This was due to fluctuation in the angular location of the transition boundary arc during the experimental run. The results in Fig. 5a show that the 20-mesh screen surface gave fractions with the shortest average fiber length as compared with the other mesh screens.

Figure 5b plots the average fiber length of cumulative collected fractions against the cumulative percentage of fiber collected from the six zones. From the results in Fig. 5b, it is clear that the 20-mesh screen surface provided excellent fiber fractionation. For example, in a single pass, the 20-mesh cone separated 8.0% of the feed fibers (a combination of Zones 4, 5, and 6)—with a combined average length of 0.78 mm—from a feed with an average length of 1.37 mm. Comparison of ΔL_L values (in the legend of Fig. 5b) for the different levels of surface roughness shows that the extent of fractionation improved in the following order: smooth < 12 mesh < 32 mesh < 20 mesh.

In earlier work *(1)*, 20-mesh and 32-mesh screens showed good fractionation of hardwood fibers (L_L = 0.75 mm). However, the current fractionation results for softwood fibers (L_L = 1.37 mm) indicates that the optimum roughness was the 20-mesh screen. Both observations suggest that the optimum roughness for the best fractionation performance may depend on the average fiber length of the feed.

Effect of cone angle

The 20-mesh screen surface provided the best fiber fractionation. Consequently, the effect of cone angle was studied using a 20-mesh screen surface. The cones used in these experiments were of 180-mm diameter with cone angles of 15°, 30°, 45°, or 60°. Tests were carried out at a rotational speed of 450 rpm for flow rates of 4.2 or 7.0 $\times 10^{-5}$ m^3/s. Fiber fractionation results for the two flow rates are shown in **Figs. 6 and 7**, respectively.

In general, for all of the cone angles used in this study, the average fiber length decreased continuously

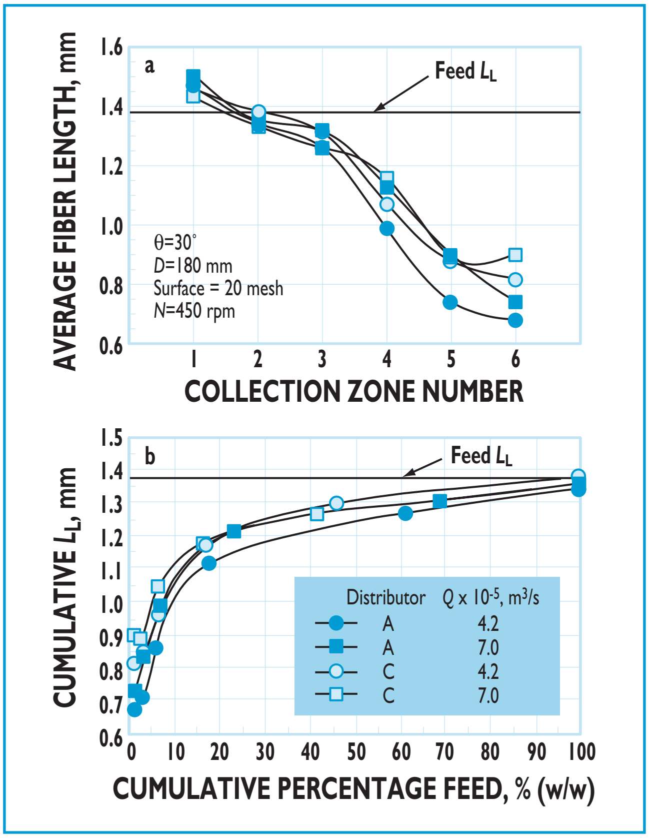

8. a: ***Average fiber length in the six collection zones and*** b: ***fractionation performance for feed distributors A and C***

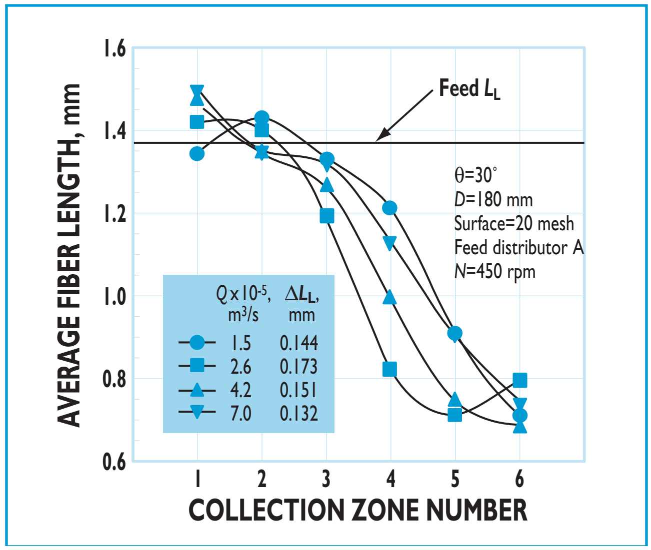

9. Average fiber length in the six collection zones at various feed flow rates

In general, for all of the cone angles used in this study, the average fiber length decreased continuously from Zone 1 to Zone 6, as seen in Figs. 6a and 7a. The lowest values of average fiber length for all zones were obtained with the 30° cone angle. At the lower feed flow rate of 4.2×10^{-5} m^3/s (Fig. 6a), the average fiber length of Zone 1 increased marginally with increasing cone angle, and the maximum value (1.6 mm) was obtained at a cone angle of 60°. Similar trends were observed at the higher flow rate of 7×10^{-5} m^3/s (Fig. 7a).

The fractionation performance of different cone angles was also evaluated by plotting the average fiber length of cumulative collected fractions against the cumulative percentage of fiber collected from the six zones, as seen in Figs. 6b and 7b. The 30° cone angle clearly gave superior fractionation performance. The high ΔL_L values in the legends of Figs. 6b and 7b confirm this observation.

Effect of feed distributor design

The effect of feed distributor design on fiber fractionation performance was studied using a 180-mm-diam. cone with a 30° cone angle and a 20-mesh screen surface. In general, at a constant feed flow rate, the feed velocity through the distributor depends on its opening area. The feed velocity increases with decreasing distributor area. When the feed suspension strikes the rotating cone surface at a higher velocity, several fountains of the feed suspension directly splash back into the collection zones close to the feed location, thus reducing fractionation performance. This phenomenon limits the maximum feed flow rate for a given distributor area. In the present study, the feed velocities at the flow rates of 2.6 and 4.2×10^{-5} m^3/s were found to be suitable for the two elliptical distributors A (area = 80 mm^2) and B (area = 35 mm^2). However, for distributor B, the feed velocity at the flow rate of 7.0×10^{-5} m^3/s was sufficiently high for splashing to occur on the cone surface. Therefore, at a given flow rate, the opening area of the distributor should be sufficiently large to avoid splashing. Fractionation performance was found to be practically the same for distributors A and B under similar experimental conditions.

The effect of the distributor shape on fractionation performance was evaluated by conducting experiments with elliptical distributor A and circular distributor C. The opening areas for distributors A and C were 80.0 and 78.5 mm^2, respectively. The radial location of the distributors was 30 mm away from the axis of rotation. The major axis of the elliptical distributor was aligned with the axis of rotation. Comparison was made at flow rates of 4.2 and 7.0×10^{-5} m^3/s at a rotational speed of 450 rpm.

Fiber fractionation results obtained with the two feed distributors are plotted in **Fig. 8**. The variation of the average fiber length with zone location was similar for both distributors, as seen in Fig. 8a. At a flow rate of 4.2×10^{-5} m^3/s, the lowest average fiber length obtained (Zone 6) with the elliptical distributor (A) was smaller than that obtained with the circular distributor (C). A comparison based on the cumulative fractions collected (Fig. 8b) shows that the elliptical distributor provided a little improvement in the fractionation performance over the cir-

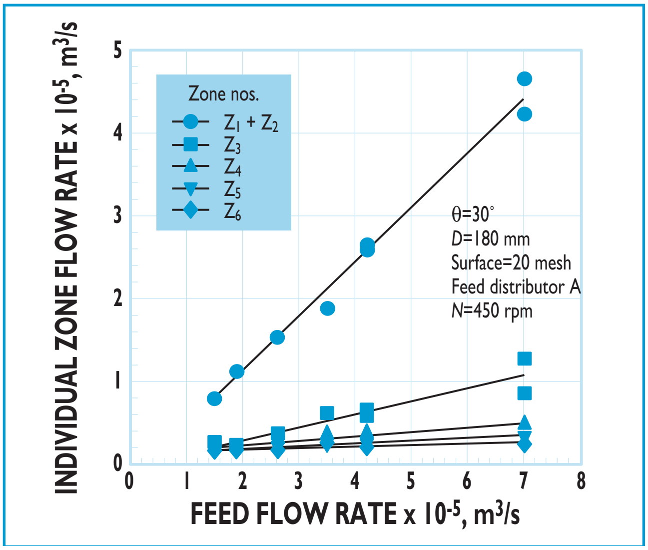

10. Individual zone flow rate as a function of feed flow rate

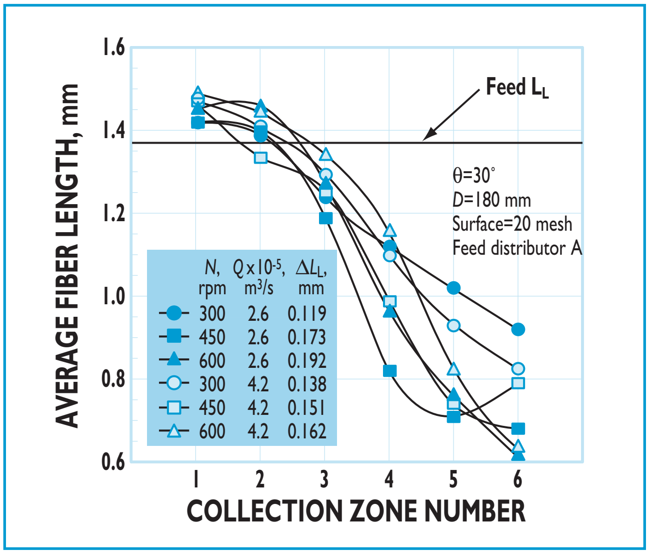

11. Average fiber length in the six collection zones at various rotational speeds and feed flow rates

cular distributor, which had nearly the same opening area.

Effect of feed flow rate

The effect of feed flow rate on fiber fractionation performance was studied using a 180-mm-diam. cone with a 30° cone angle and a 20-mesh screen surface. The flow rate was varied from 1.5 to 7.0 × 10^{-5} m^3/s at a rotational speed of 450 rpm.

Figure 9 shows the variation of average fiber length within the six collection zone at various flow rates. The results show that fractionation performance was better at flow rates of 2.6 and 4.2 × 10^{-5} m^3/s as compared with the flow rates of 1.5 and 7.0 × 10^{-5} m^3/s. The value of ΔL_L (in legend of Fig. 9) was highest (0.173 mm) for a flow rate of 2.6 × 10^{-5} m^3/s, indicating a more effective fiber fractionation.

In general, with an increase in the feed flow rate, the residence time of a suspension on the cone surface decreases, and the tendency for film formation along the rim of the cone increases *(1)*. The result is a reduction in fractionation performance at a high flow rate (7.0 × 10^{-5} m^3/s). However, at a very low rate (1.5 × 10^{-5} m^3/s), the incoming feed suspension overlaps with the fractionated suspension on the cone surface, which also reduces the fractionation performance. Therefore, for a given cone rotational speed, there is an optimum flow rate for the best fractionation performance.

Figure 10 shows the variation in the flow rate into individual collection zones with respect to the feed flow rate. In general, at a constant rotational speed, increasing the feed flow rate increases the fractional fraction flow rate into an individual zone. However, the extent of the increase was found to decrease substantially after Zone 3. This suggests that increasing the feed flow rate does not substantially increase the throughput in Zones 4, 5, and 6.

Effect of rotational speed

The effect of cone rotational speed on fiber fractionation performance was studied using a 180-mm-diam. cone with a 30° cone angle and a 20-mesh screen surface. Rotational speed was varied from 300 to 600 rpm. Tests were carried out at flow rates of 2.6 and 4.2 × 10^{-5} m^3/s. The fiber fractionation results in **Fig. 11** show that the extent of fractionation (values of ΔL_L in legend of Fig. 11) improved substantially with an increase in the rotational speed from 300 to 450 rpm. However, with a further increase in rotational speed from 450 to 600 rpm, the fractionation performance improved only slightly. In our earlier work on hardwood fiber fractionation *(1)*, we found that, for a given flow rate, there is an optimum rotational speed for the best fractionation performance.

The influence of cone rotational speed on the flow rates into the six individual zones of the collection assembly was also studied. **Figure 12** shows the variation of the flow rate into the six zones with increasing rotational speed at a constant flow rate of 4.2 × 10^{-5} m^3/s. The results show that with increasing rotational speed, the flow rates into Zones 1 and 2 decrease while the flow rates into Zones 3, 4, 5, and 6 increase. However, the increase in the flow rates for Zones 4, 5, and 6 was marginal. This suggests that increasing the cone rotational speed does not increase the throughput into Zones 4, 5, and 6.

Scale-up

Preliminary tests were conducted to investigate scale-up of a rotating cone fractionator at a constant flow rate of 2.6 × 10^{-5} m^3/s. Cones (30° cone angle, 20-mesh surface roughness) of 120-mm and 180-mm diameter were rotated at 670 and 450 rpm, respectively. **Figure 13** shows the fiber fractionation results. The variation in fiber length with zone location was the same for both cones, as

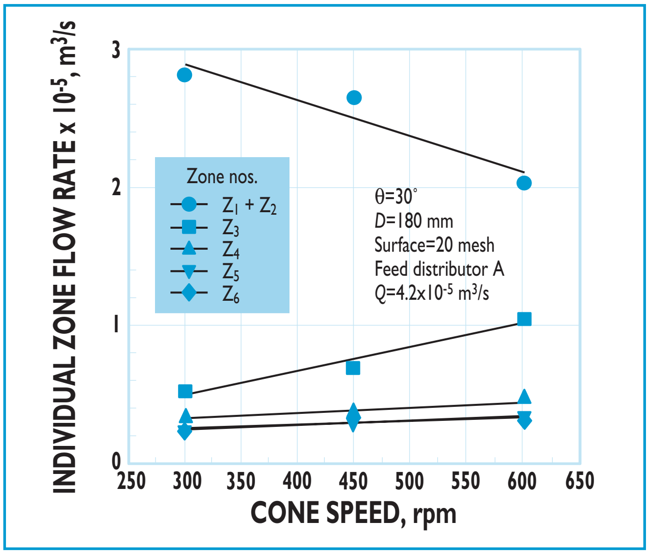

12. Individual zone flow rate as a function of cone rotational speed

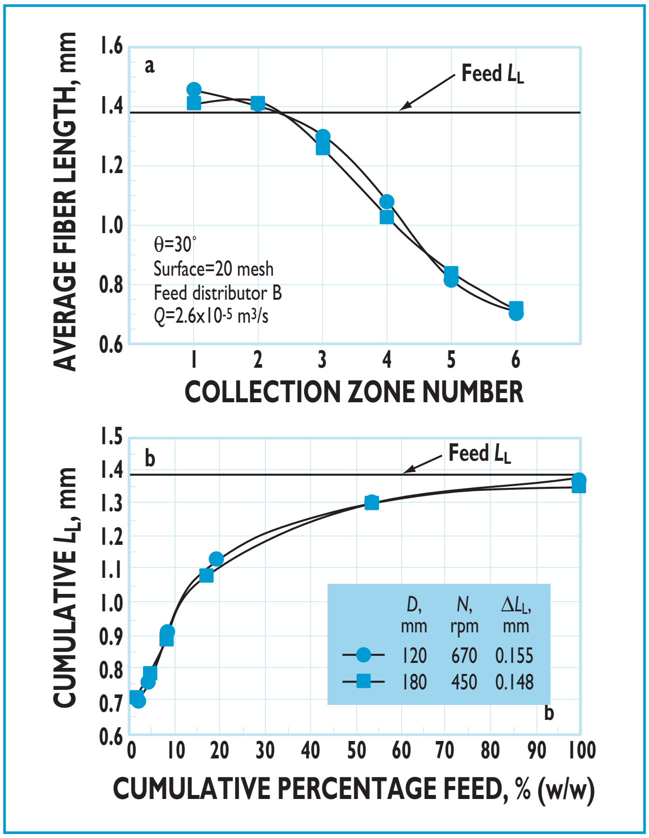

13. a: ***Average fiber length in the six collection zones and*** b: ***fractionation performance for two combinations of cone diameter and rotational speed***

seen in Fig. 13a. Similarly, a comparison based on the cumulative fractions collected (Fig. 13b) shows that both cones provided similar fractionation performance. The values of ΔL_L for the 120- and 180-mm diameter cones were 0.155 and 0.148 mm, respectively, also indicating similar fractionation performance. The rotational speeds for the two cones were selected in such a way that the ratio of their tip speeds was constant. At a given flow rate, the fractionation performance for the two cones was similar, suggesting the possibility of scale-up on the basis of constant tip speed. However, a detailed investigation is in progress to develop suitable scale-up criteria for the rotating cone fractionator.

CONCLUSIONS

A laboratory study of a rotating-cone fractionator led to the following conclusions:

1. Fractionation performance was improved by aligning the first zone of the collection assembly with the dispersed spray originating from the transition boundary at the cone rim.
2. A rotating cone with a rough surface gave better fiber fractionation performance than a rotating cone with a smooth surface. In the present study, a roughness of 20-mesh sieve provided the best fiber fractionation performance.
3. A cone angle of 30° gave the best fractionation performance.
4. The design of the feed distributor influenced fiber fractionation performance. An elliptical feed distributor, with a large opening area placed off-center to the axis of rotation, gave slightly better fiber fractionation performance than a circular distributor.
5. Flow rates into Zones 4, 5, and 6 (shortest fiber lengths) were insensitive to the feed flow rate and cone rotational speed.
6. At constant flow rate, the rotational speed required to achieve a similar fractionation performance decreased with increasing cone diameter. The current results indicate a scale-up criterion based on a constant tip speed. However, a detailed investigation is necessary to substantiate this. **TJ**

Rewatkar is a research associate and Masliyah is a professor of chemical engineering in the Dept. of Chemical and Materials Engineering, 536 Chemical-Mineral Engineering Building, University of Alberta, Edmonton, AB, Canada T6G 2G6.

V.B.R. gratefully acknowledges the financial support of the Natural Sciences and Engineering Research Council of Canada (NSERC International Fellowship) and the Excellence in Mechanical and Chemimechanical Wood Pulps Network. The authors thank William Eckert and David Zoobkoff for their help.

Received for review Aug. 7, 1997.

Accepted March 22, 1998.

NOMENCLATURE

D = cone diameter, mm
h_f = vertical height of feed pipe (as shown in Fig. 3), mm
L = fiber length, mm
L_A = arithmetic mean fiber length, mm
L_L = length-weighted mean fiber length, mm
L_{LF} = length-weighted mean fiber length of all six zones (as defined by Eq. 4), mm
L_W = weight-weighted mean fiber length, mm
ΔL_L = extent of fractionation, mm
n = fiber count
N = cone rotational angular velocity, rpm
Q = volumetric flow rate of feed suspension, m^3/s
r = distance in the radial direction from the axis of rotation, mm
r_f = radial distance of feed pipe from the axis of rotation (as shown in Fig. 3), mm
x_i = weight fraction of feed fibers collected in *i*th zone
X = consistency of pulp, % w/w
Z_1 to Z_6 = zone numbers of collection assembly
α = angle between angular location of feed pipe and transition boundary (as shown in Fig. 2a), degrees
θ = cone angle (as shown in Fig. 3), degrees

LITERATURE CITED

1. Rewatkar, V. B. and Masliyah, J. H., *Can. J. Chem. Eng.* 75(1): 196(1997).
2. Moller, K., de Ruvo, A., Norman, B., *et al.*, *Paper Technol.* 20(3): 100(1979).
3. Moller, K., Duffy, G. G., Moller, J. T., *et al.*, *Tappi* 63(9): 89(1980).
4. Duffy, G. G., Pedersen, M. L., and Petersen, J. H., *Appita* 35(6): 512(1982).
5. Oroskar, A. R., "Spray fractionation," Ph.D. thesis, University of Wisconsin–Madison, Madison, 1981.
6. Oroskar, A. R. and Crosby, E. J., U.S. pat. 4,427,541 (1984).
7. Klungness, J. H., Oroskar, A. R., and Crosby, E. J., *Tappi J.* 67(6): 78(1984).
8. Oroskar, A. R. and Crosby, E. J., *I&EC Fundam.* 25(4): 483(1986).
9. Rewatkar, V. B. and Masliyah, J. H., "Wood pulp fiber fractionation," in "Mixed-flow hydrodynamics," *Advances in Engineering Fluid Mechanics Series* (N. P. Cheremisinoff, Ed.), Gulf Publishing, Houston, 1996, p. 871.
10. TAPPI T 240 om-88 "Consistency (concentration) of pulp suspensions."